

## PROBLEMS IN THE DETECTION OF QUASI-RECTANGULAR MAGNETIC FLUX DENSITY WAVEFORMS

*D. Giordano, G. Crotti*

Istituto Nazionale di Ricerca Metrologica, Torino - Italy  
d.giordano@inrim.it

**Abstract:** The paper focuses on the distortions introduced by low frequency magnetic field meters in the measurement of pulsed or periodic quasi-rectangular waveforms, such as those experienced near welding devices or Magnetic Resonance Imaging (MRI) machines. Starting from the meter frequency response, evaluated by generating reference sinusoidal magnetic fields up to a hundred of hertz, a circuital model is worked out, which reproduces the distortions of the measured signal due to the meter input high pass filter. By making use of the modelled filter, a time domain reconstruction procedure is implemented that allows the reproduction of the actual magnetic field shape starting from the measured behaviour.

**Key words:** Magnetic fields, measurement, signal distortion, welding.

### 1. INTRODUCTION

The assessment of human exposure to low frequency time-varying magnetic fields is, in the first instance, quite always based on measurements generally performed by field meters equipped with three-axial induction probes. In the case of sinusoidal magnetic fields, compliance with the exposure limits is directly verified by comparison with the prescribed magnetic flux density reference levels, which are expressed as r.m.s. values as a function of the frequency [1]. In the presence of distorted waveforms, the exposure levels are determined by evaluating the different contributions in the frequency domain or by making use of suitable complex weighting functions [2, 3]. The exposure evaluation is then strictly dependent on the meter capability of detecting the actual field waveform.

Measurements carried out by making use of meters that output the analog behaviour of the three orthogonal field components show that distortions are introduced in the case of pulsed and periodic quasi-rectangular/trapezoidal magnetic fields. The shape of such fields is characterised by rump up and rump down times up to hundreds of microseconds and flat top up to hundreds of milliseconds. In the following, the response of commercial field meters to quasi-rectangular magnetic flux densities is investigated by making reference to field waveforms experimented in on-site situations. Starting from the analysis of the meter output frequency response, evaluated by generating reference

sinusoidal magnetic fields by a Helmholtz coil system, circuital models are developed, to reproduce the distortions of the measured signal that can be ascribed to the presence of the meter input high pass filter. By making use of the implemented filter model, a procedure is worked out to reconstruct the actual magnetic fields waveforms starting from the field meter outputs.

### 2. QUASI-RECTANGULAR WAVEFORMS

With reference to the evaluation of workers exposure, devices that produce magnetic fields generated by currents with pulsed or periodic quasi-rectangular waveforms with frequency spectrum up to several tens of kilohertz can be met near welding devices and close to Magnetic Resonance Imaging (MRI) machines. In the first case, the current which flows during the welding operation is cyclically switched on and off. The resulting current is a sequence of rising and decreasing exponential behaviours, broken by constant current intervals, which give rise to a quasi-rectangular waveform. The same time behaviour is expected for the generated magnetic field.

As an example, the magnetic flux density and the current shapes simultaneously recorded during a welding sequence are shown in Fig. 1. The current is measured by a Rogowski coil, whereas a meter equipped with analog outputs is used for the field detection. As can be seen, the measured magnetic flux density is quite different from the current during the time intervals characterized by a constant current value.

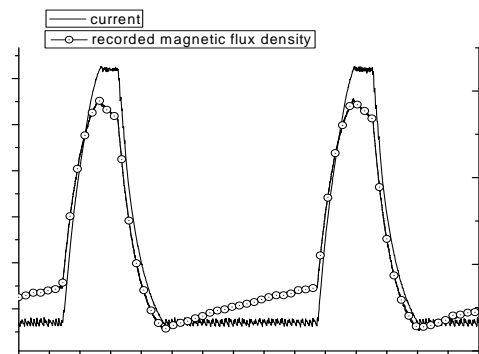


**Fig. 1. Comparison between current and magnetic flux density time behaviours simultaneously recorded during a welding operation.**

Since the exposure levels depend on the field amplitude and on its frequency content [1, 2, 3], an unfaithful reproduction of the field shape can lead to an inaccurate exposure assessment.

A similar current flows in the MRI gradient coils, which are used to produce controlled linear gradient fields in the main static magnetic field, for body slice selection and phase/frequency encoding [4, 5]. In this case, the resultant magnetic field waveform can be far more different from the current one, because it is the combination of contributions due to different sets of coils, in which trapezoidal and/or not in phase currents flow.

## 2. ANALYSIS OF THE DISTORTION INTRODUCED

### 2.1. Magnetic flux density meter

The environmental low frequency time-varying magnetic flux density is usually detected by means of meters, whose sensor is made of three orthogonal coils, with bandwidth up to some hundreds of kilohertz. The magnetic flux density components are obtained by integrating the voltage induced across the coils. A high pass filter (HPF), whose cut-off frequency is set at a very low frequency (from a few hertz to some tens of hertz), is inserted at the input stage before the signal integration (Fig. 2). As known, it allows both the removal of the unavoidable d.c. component that is introduced by the conditioning circuits and the mitigation of the stray voltage induced across the coils, due to possible coil vibrations.

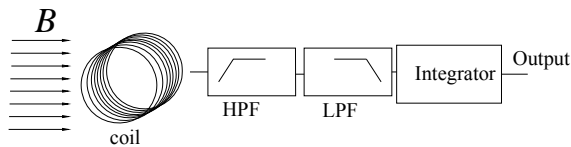


Fig. 2. Simplified scheme of a low frequency magnetic flux density meter, which includes the HPF and the low pass filter (LPF).

### 2.1. First-order model of the HPF

The incorrect reproduction of the field shape can be attributed to the high pass filter (HPF) in the signal processing chain (Fig. 2). To underpin this statement, a simple model which includes the coil and a first order HPF is implemented in Matlab-simulink<sup>®</sup> environment. The presence of the LPF is not considered, because the frequency spectrum of the field shapes of interest is well below the cut-off frequency of the used meters.

A measurement set-up is then arranged to check the validity of the modelled filter. It involves a Helmholtz coil system for the generation of reference magnetic fields up to 100 kHz [6], a power supply composed of an arbitrary waveform generator and a power amplifier, a calibrated field meter that outputs three analog signals proportional to the detected magnetic flux density components (LPF cut-off frequency 400 kHz) and a digital sampling oscilloscope.

The current flowing in the Helmholtz coils (Fig. 3) is set to reproduce, quite faithfully, the actual waveform absorbed by an arc welding device [7]. It is made of a rising and a descending exponential behaviour, linked by a 1 ms flat part. The meter filter, which can be selected by the user, is

set at 10 Hz. As shown in Fig. 3, the model output reproduces quite well the measured field. However, this is no longer valid in the case of flat current durations longer than the time constant of the RC filter ( $\tau = 6.5$  ms). A proof of that is shown in Fig. 4 where the comparison between computed and measured meter output signals is shown under a rectangular magnetic flux density with 3 Hz repetition frequency.

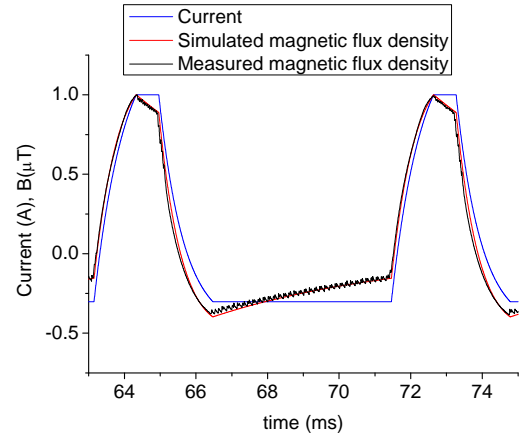


Fig. 3. Simulated meter output and measured magnetic flux density in the Helmholtz system supplied by the quasi-rectangular current.

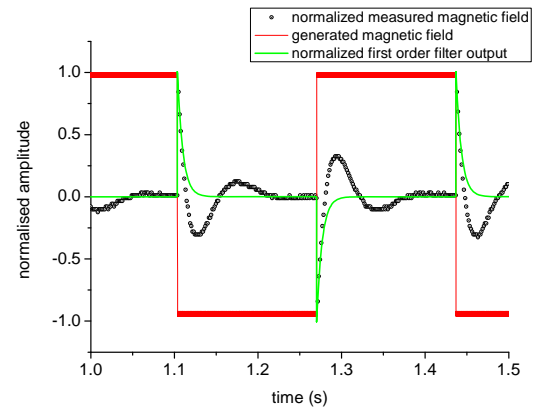


Fig. 4. Simulated and measured meter output signal under a rectangular magnetic field stimulus with a frequency of 3 Hz. All the quantities are normalized to their peak value.

### 2.2. Investigation on the actual filter

An analysis addressed to the estimation of the meter frequency response is carried out in order to implement a HPF filter that better approximates the effects of the actual one. The transfer function of the field meter, whose simplified scheme is shown in Fig. 2, is experimentally assessed from 5 Hz to 100 Hz. The set up is the same employed for the assessment of the validity of the first order model. In addition, a phase meter is used for the detection of the phase displacement between the signal coming from the magnetic flux density probe and the coil current, obtained by measuring the voltage drop across a calibrated non inductive resistor series connected to the Helmholtz coils. Since the transfer function of the sensing coils, which has a derivative effect, and the integrator cancel each other and

the LPF becomes effective at higher frequencies, the overall measured transfer function can be assumed to be equivalent to the HPF one. Figure 5 shows the frequency behaviour of the transfer function gain and phase displacement. It highlights some interesting characteristics. First, the flatness of the magnitude for high frequency rules out a Chebyshev and a Causer architecture for the investigated filter; secondly, the cut-off frequency is slightly different from the selected one (10 Hz) and finally the magnitude behaviour, which increases with a slope of 60 dB/dec at low frequency, and the phase total variation, which is  $270^\circ$ , let us assume that it is a third order filter.

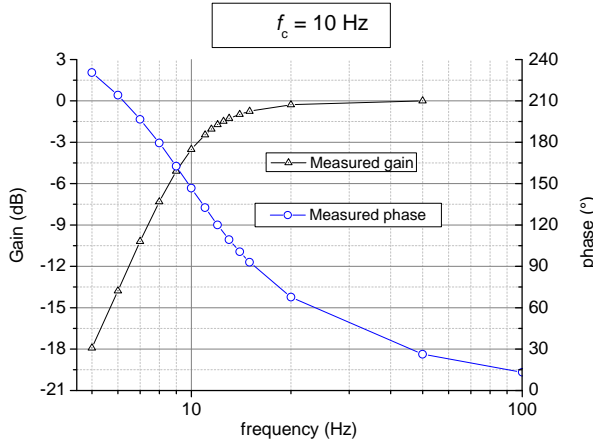


Fig. 5. Measured gain and phase of the meter transfer function versus frequency.

### 2.3. High pass filter model

On the basis of the frequency behaviour experimentally detected, a third order Butterworth filter architecture is chosen as a first attempt. Figure 6 shows the electric circuit associated with the stated filter connected to a resistive load.

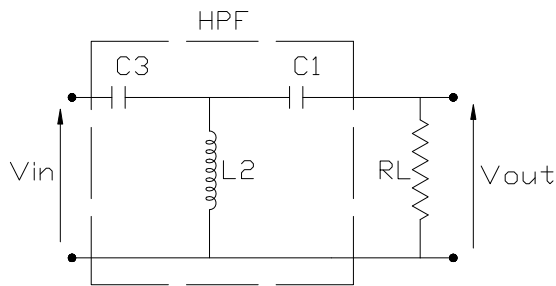


Fig. 6. Scheme of the HPF electrical model and the load (RL).

As well known, the values of inductance L2 and capacitances C1 and C3 are normalized for a cut-off angular frequency  $\omega_c=1$  rad/s and a load of  $RL=1 \Omega$ . To set the cut-off angular frequency at  $\omega_c = 2\pi f_c$  with  $f_c = 10$  Hz, the electric parameters are divided by  $\omega_c$ . Table I gives the values of inductance and capacitances which make the filter for the cut-off frequency of 10 Hz and 30 Hz.

Clearly, the assigned inductive and capacitive parameters cannot be the values implemented in the actual

filter. Nevertheless, they allow a quite satisfactory approximation of the frequency response, as shown in Fig. 7 where the computed and measured frequency behaviours are compared.

Table I. Value of the filter electrical parameters for  $RL=1 \Omega$

$f_c$	C1	L2	C3
10 Hz	32 mF	12 mH	10.6 mF
30 Hz	10.6 mF	3.98 mH	3.54 mF

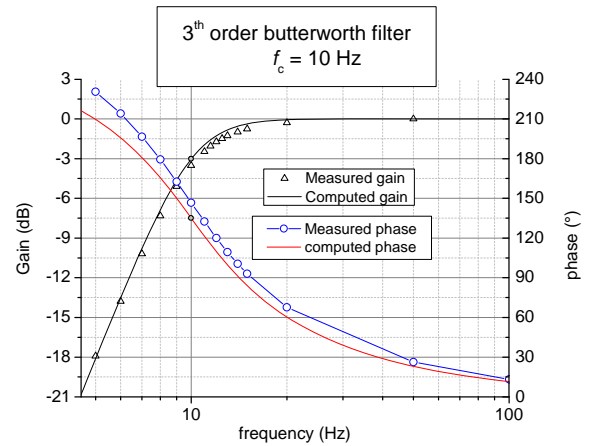


Fig. 7. Comparison between measured and computed gain and phase of the HPF with 10 Hz cut-off frequency.

Even though the actual cut-off frequency is slightly higher than the rated 10 Hz, the comparison shows a reasonable reproducibility of the actual frequency behaviour. The highest discrepancy (about  $20^\circ$ ) is recorded for the phase at very low frequency that reduces to  $3^\circ$  at 50 Hz. This can be due to the difficulty in the detection of the phase delay at these low frequencies, where the voltage amplitude is strongly reduced by the filter presence. The same procedure is repeated for a cut-off frequency of 30 Hz (Fig. 8).

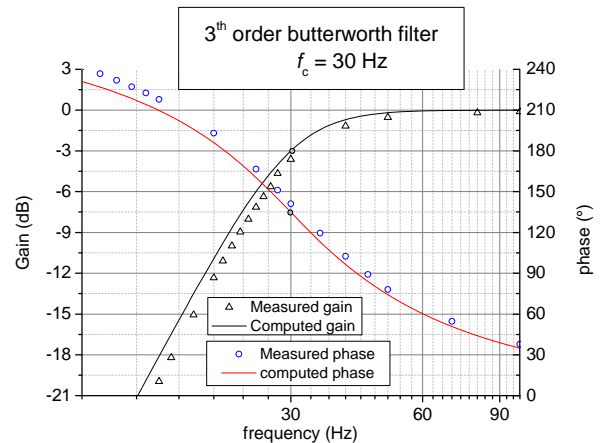


Fig. 8. Comparison between measured and computed gain and phase of the HPF with 30 Hz cut-off frequency.

The considerations relevant to the 10 Hz cut-off frequency filter do also apply to the 30 Hz case, but a more significant deviation between measured and computed gain is found at low frequency. This deviation can be explained by considering that the actual values of the meter input filter parameters, which are clearly unknown, may slightly differ from the Butterworth filter values.

### 2.3. Model effectiveness in the time domain

The effectiveness of the filter model is experimentally validated. The output voltage given by the meter under a square magnetic flux density stimulus at 3 Hz, 12 Hz and 50 Hz is compared to the model output obtained with the same stimulus. To this end, a square voltage is generated by the arbitrary waveform generator. Because of the low frequency and the limited total inductance of the system, the current flowing in the Helmholtz coil pair could be considered quasi-rectangular. However, a simple circuit model of the magnetic flux density generation circuit is introduced to carry out the comparison between computations and measurements under the same conditions. Figure 9 shows the results of the comparison between measured and simulated response with a HPF cut-off frequency of 10 Hz for the three considered frequencies.

The reliability of the HPF model is confirmed by the quite satisfactory agreement between computation and measurement. The not complete overlap of the two curves, which was already found in the frequency domain, may be also partially charged to the discrepancy between actual and rated value of the filter parameters.

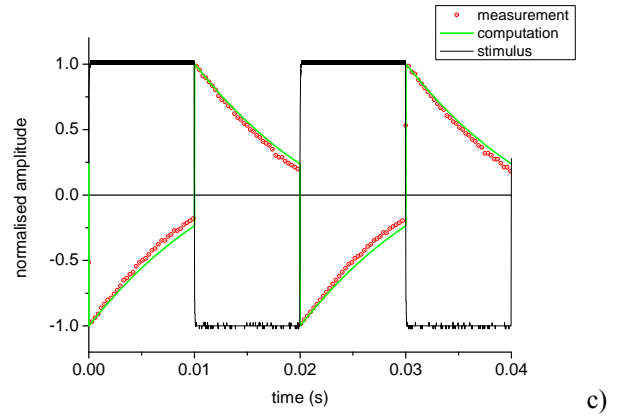
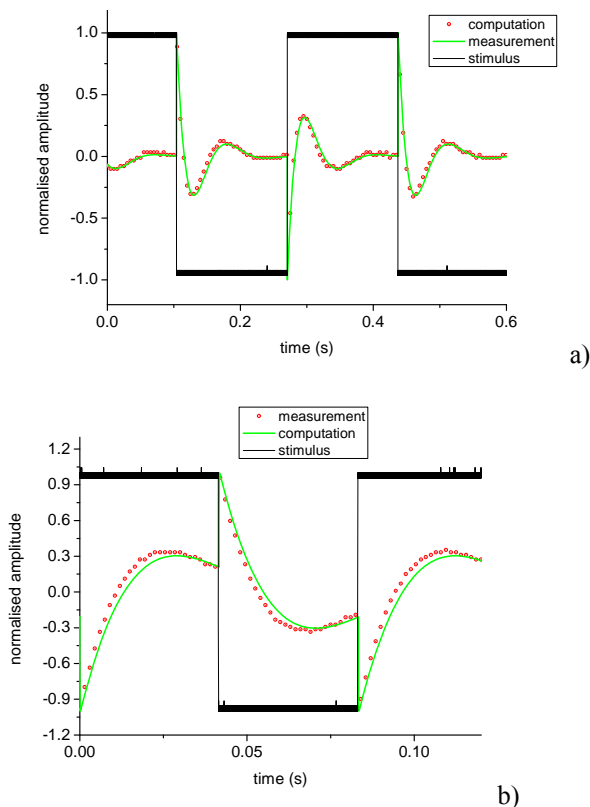


Fig. 9. Measured and computed meter outputs (values normalised to their peak), under a 3 Hz (a), 12 Hz (b) and 50 Hz (c) quasi-rectangular field.

The filter model is further experimentally verified by generating an input signal proportional to the magnetic field produced by the current waveform absorbed by a resistive welding device. The magnetic flux density was measured 10 cm far from the handle. The supply current (Fig. 10) has a quasi-rectangular waveform, which lasts about 0.7 s, with a superimposed ripple not shown in Fig. 10. The output meter waveform shows two damped oscillations; the second one is the free filter response, since it is generated by the switching off of the supply current (Fig. 10).

This difference is stronger than that shown in the behaviour of Fig. 9a, even if the stimulus is quite similar. This fact may be explained by supposing a non-linearity of the inductive filter parameters, since the amplitude of the magnetic flux density is, in the case of the field generated by the resistance-welding device, of the order of several hundreds of microtesla, whereas it is no more than some microtesla in the previously investigated situations.

Figure 11, which gives the comparison between measurement and computation, highlights a difference in the amplitude and frequency oscillation of the free filter response.

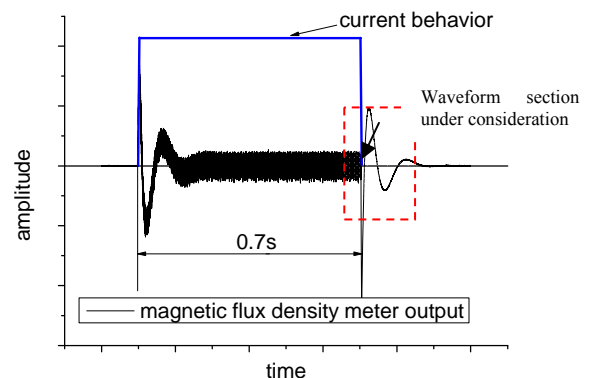


Fig. 10. Magnetic flux density detected near a cable supplied by a quasi-rectangular current.

This difference is stronger than that shown in the behaviour of Fig. 9a, even if the stimulus is characterized by similar rump up and rump down times. This fact may be explained by supposing a non-linearity of the inductive filter

parameters since the amplitude of the magnetic flux density is in the case of the field generated by the resistance welding device of the order of several hundreds of microtesla whereas it is no more than some microtesla in the laboratory investigated situations.

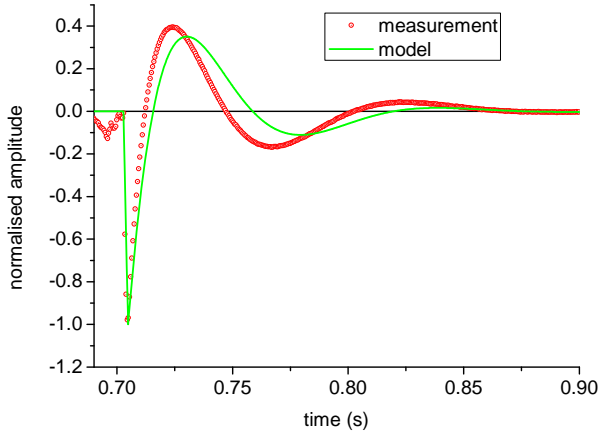


Fig. 11. Measurement and computation comparison for the free filter response.

### 3. CORRECTION PROCEDURE FOR THE FILTER DISTORTION

As a last step, a numerical procedure is worked out to reconstruct the actual magnetic flux density behaviour applied to the probe, starting from the voltage signal output by the meter. To this end, the electrical circuit shown in Fig. 12 is considered, where the known quantity is the voltage drop  $v_{out}(t)$  across the unitary resistance  $RL$ , and the unknown is the voltage  $v_{in}(t)$  that is proportional to the magnetic field to be determined.

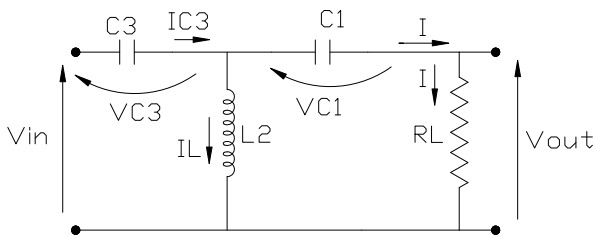


Fig. 12. Electrical circuit for the input voltage  $V_{in}$  reconstruction procedure.

The reconstruction procedure involves the sequential solution of a series of equations, which entail the time integration of the current which flows in the resistance  $RL$ , the inductance  $L2$  and the capacitance  $C3$ . It is implemented in matlab<sup>®</sup> environment according to the block scheme shown in Fig. 13. Since the considered waveforms have zero mean value, the integration constants are implicitly defined by zeroing the dc component of the integrated quantities.

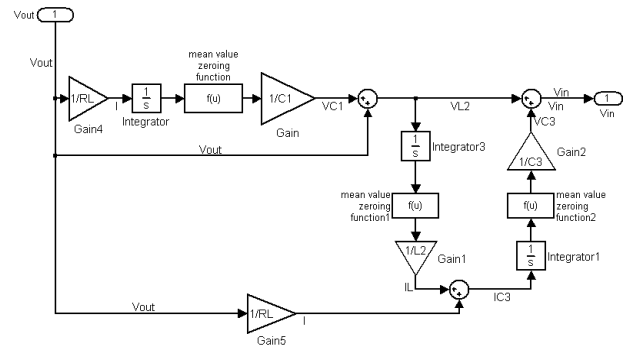


Fig. 13. Block scheme of equation solution

A numerical test of the correction procedure is performed by comparing the enforced quasi-rectangular input waveform with the one reconstructed from the filter model output (see Fig. 14). As a stricter verification, the correction procedure is applied to the measured behaviour of an actual magnetic flux density generated by the Helmholtz coil system. Fig 15 shows that the reconstructed magnetic field reproduces quite well the shape of the coil current and so the applied magnetic flux densities.

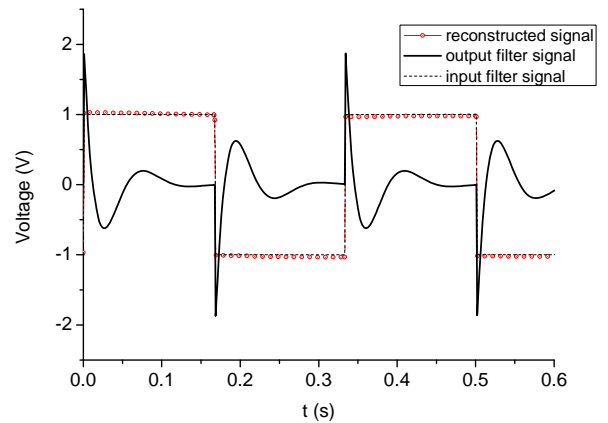


Fig. 14. Comparison between the enforced and reconstructed input filter signal.

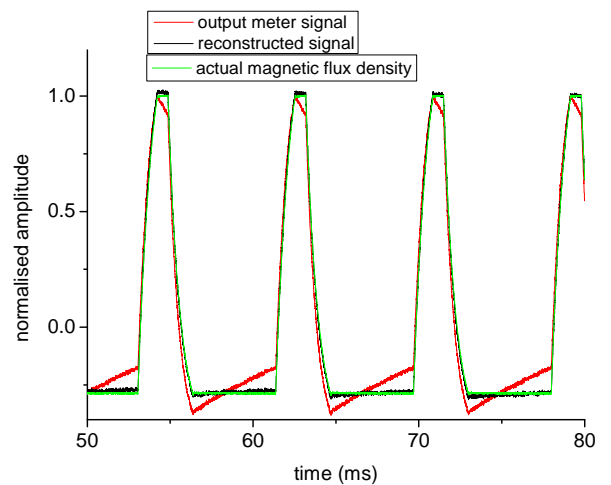


Fig. 15. Comparison between the actual magnetic flux density and the one reconstructed from the output meter signal.

#### 4. CONCLUSION

Critical points in the detection of quasi-rectangular magnetic flux densities for dosimetric aim are put in evidence. The actual output of a low frequency commercial meter is laboratory reproduced by implementing semi-empirical models of its input filter, with increased complexity of the signal conditioning chain. By making use of a third order Butterworth HPF model the actual magnetic field waveform experienced by the investigated meter is reconstructed from the measured field behaviours. The effectiveness of the developed procedure is proved by the comparison between the reconstructed magnetic flux density and the imposed one. The filter model will be completed by introducing a non-linearity of the inductive parameter, to improve its efficiency in presence of high magnetic flux densities. The proposed approach can be extended to other field meters with different input high pass filters, provided that their complex frequency behaviour is assessed.

#### REFERENCES

- [1] ICNIRP “Guidelines for limiting exposure to time-varying electric and magnetic fields (1 Hz to 100 kHz)”, Health Physics, December 2010, Volume 99, No 6.
- [2] ICNIRP Statement “Guidance on Determining Compliance of Exposure to Pulsed Fields and Complex Non-Sinusoidal Waveforms below 100 kHz with ICNIRP Guidelines”, Health Physics 84 (3): 383-387; 2003.
- [3] 4. Jokela K., “Restricting exposure to pulsed and broadband magnetic fields”, Health Physics, vol. 79, n. 4, pp. 373-388 (2000).
- [4] Guofa Shou et Al. “MRI coil design using Boundary element Method Technique: A numerical calculation study”, IEEE Trans. on MAG, Vol. 46, no. 4, pp. 1052-1059, 2010.
- [5] M. Capstick et al. Report on Project VT/2007/017 “An Investigation into Occupational Exposure to Electr. Fields for Personnel Working With and Around Medical MRI Equipment”, 4 April 2008.
- [6] M. Chiampi, G. Crotti, D. Giordano “Set up and characterization of a system for the generation of reference magnetic fields from 1 to 100 kHz”, IEEE Trans. on IM, Vol. 564, no. 2, pp. 300-304, 2007.
- [7] P. Mair, “Assessment of EMF (Electromagnetic fields) and biological effects in ARC welding applications”, International Institute of Welding, Commission XII, Intermediate Meeting, Fronius International, Feb. 2005.